Silencing of *microRNA-122* is an early event during hepatocarcinogenesis from non-alcoholic steatohepatitis

Yoko Takaki,[1] Yoshimasa Saito,[1,2] Azusa Takasugi,[1] Kohta Toshimitsu,[1] Shoji Yamada,[1] Toshihide Muramatsu,[1] Masaki Kimura,[1] Kazuo Sugiyama,[2] Hiromu Suzuki,[3] Eri Arai,[4] Hidenori Ojima,[4] Yae Kanai[4] and Hidetsugu Saito[1,2]

[1]Division of Pharmacotherapeutics, Keio University Faculty of Pharmacy, Tokyo; [2]Division of Gastroenterology, Department of Internal Medicine, Keio University School of Medicine, Tokyo; [3]Department of Molecular Biology, Sapporo Medical University, Sapporo; [4]Division of Molecular Pathology, National Cancer Center Research Institute, Tokyo, Japan

Non-alcoholic steatohepatitis (NASH) has emerged as a common cause of chronic liver disease and virus-independent hepatocellular carcinoma (HCC) in patients with obesity, diabetes, and metabolic syndrome. To reveal the molecular mechanism underlying hepatocarcinogenesis from NASH, microRNA (miRNA) expression profiles were analyzed in STAM mice, a NASH-HCC animal model. MicroRNA expression was also examined in 42 clinical samples of HCC tissue. Histopathological images of the liver of STAM mice at the ages of 6, 8, 12, and 18 weeks showed findings compatible with fatty liver, NASH, liver cirrhosis (LC), and HCC, respectively. Expression of *miR-122* in non-tumor LC at the age of 18 weeks was significantly lower than that in LC at the age of 12 weeks. Expression of *miR-122* was further decreased in HCCs relative to non-tumor LC at the age of 18 weeks. Expression of *miR-122* was also decreased in clinical samples of liver tissue showing macrovesicular steatosis and HCC, being consistent with the findings in the NASH model mice. DNA methylation analysis revealed that silencing of *miR-122* was not mediated by DNA hypermethylation of the promoter region. These results suggest that silencing of *miR-122* is an early event during hepatocarcinogenesis from NASH, and that *miR-122* could be a novel molecular marker for evaluating the risk of HCC in patients with NASH.

Hepatocellular carcinoma is the most common type of liver cancer. Most cases of HCC are secondary to either chronic hepatitis or liver cirrhosis caused by viral infection (hepatitis B or C) or alcoholism. Hepatocellular carcinoma accounts for 85–90% of all primary liver cancers and is one of the most lethal, affecting many of the world's population.[1,2] Despite improvements in the treatment of viral infections, such as interferon therapy, the incidence of HCC is still increasing in parallel with the increased incidence of obesity, diabetes mellitus, and metabolic syndrome.[3] Recently, NAFLD has emerged as a common cause of chronic liver disease in patients with metabolic syndrome.[4] Non-alcoholic steatohepatitis is a more severe form of NAFLD and is defined by the presence of steatosis with inflammation and progressive fibrosis, leading to LC and HCC. Non-alcoholic steatohepatitis may account for a large proportion of virus-independent HCC in developing countries.[4,5] However, the molecular mechanism underlying hepatocarcinogenesis from NAFLD and NASH is poorly understood.

MicroRNAs are small non-coding RNAs that function as endogenous silencers of various target genes. MicroRNAs are expressed in a tissue-specific manner and play important roles in cell differentiation, proliferation, and metabolism.[6,7] Links between miRNAs and the initiation and development of cancer and metabolic disorders are becoming increasingly apparent.[7–9] We have recently reported that the important tumor suppressor miRNAs are regulated by epigenetic alterations such as DNA methylation and histone modification at their CpG island promoters.[10] Regulation of miRNAs by chromatin-modifying drugs may be a novel therapeutic approach for malignant disorders.[10–13] Despite these discoveries, little is known about the roles of miRNAs in NASH-associated hepatocarcinogenesis.

To reveal the roles of miRNAs during hepatocarcinogenesis from NAFLD and NASH, we examined miRNA expression profiles in NASH-HCC model mice. In the present study, we used STAM mice as a NASH-HCC model.[14,15] Here we show that the liver-specific *miroRNA-122* (*miR-122*) gene is downregulated at the early stage of hepatocarcinogenesis from NASH in both an animal model and samples of human tissue.

Materials and Methods

Animals and experimental design. STAM mice (Stelic Institute & Co., Tokyo, Japan) were used as a NASH-HCC model in the present study. STAM mice were established as described previously.[14] In brief, 2-day-old male C57BL/6J pups were injected with streptozotocin (200 μg per mouse) and fed

a high-fat diet (HFD-32; Clea, Tokyo, Japan) from the age of 4 weeks. This mouse model shows progression of NAFLD to NASH at 8 weeks of age, and to HCC at 18 weeks of age. A total of 14 STAM mice were purchased, and those used as a model for NAFLD, NASH, LC, and HCC were killed and dissected at the ages of 6 ($n = 4$), 8 ($n = 4$), 12 ($n = 2$), and 18 ($n = 4$) weeks, respectively. C57BL/6J mice were used as controls. Tissue samples and blood were obtained from both control and STAM mice. Histological and biochemical examinations were carried out as described previously.[16] All animals had free access to water and food and were maintained in a temperature-controlled specific pathogen-free animal facility. All experiments and procedures were approved by the Keio University Animal Research Committee.

Patients and tissue specimens. A total of 42 clinical samples of HCC were examined. Tissue specimens from HCCs and their surrounding non-tumor liver tissues were obtained from materials surgically resected from 42 patients (HCV-positive, 22; HBV-positive, 6; non-B/non-C, 14) at the National Cancer Center Hospital (Tokyo, Japan). Non-B/non-C HCC patients were further divided into two groups according to the grade of macrovesicular steatosis in the non-tumor liver tissue, as reported previously (grade 0, 5; grade 1–3, 9).[17] This study was approved by the Ethics Committees of the National Cancer Center and Keio University. Written informed consent was obtained from all of the patients.

Cell lines and drug treatment. The human liver cancer cell lines HepG2 and HuH7 were used in this study. HepG2 was obtained from Riken Cell Bank (Tsukuba, Japan), and HuH7 from the ATCC (Rockville, MD, USA). Both cell lines were cultured in DMEM (Life Technologies, Carlsbad, CA, USA) supplemented with 10% FBS, and seeded at 1×10^5 cells per 100-mm dish 24 h prior to treatment with 1 or 3 μM 5-Aza-CdR (Sigma-Aldrich St Louis, MO, USA). The 5-Aza-CdR was removed from the culture medium at 24 h, and regular medium was used thereafter.

RNA extraction and microarray analyses. Total RNAs from liver tissues of STAM mice and liver cancer cell lines were extracted using the mirVana miRNA isolation kit (Life Technologies). Total RNAs from clinical HCC samples and matched non-tumor liver tissues were extracted using TRIzol reagent (Life Technologies). MicroRNA microarray analyses were carried out by Toray Industries (Tokyo, Japan). The microarray chips used contained probe regions that detected 1135 (Toray Industries) miRNA transcripts listed in Sanger miRBase Release 17.0. Multiple probes for each miRNA were included, and the average values of their signal intensities were compared. All data were submitted to the Gene Expression Omnibus under the accession number GSE52822.

Quantitative RT-PCR of miRNA. Levels of miRNA expression were analyzed by quantitative RT-PCR using the TaqMan miRNA assay for human/mouse miR-122 (Life Technologies) in accordance with the manufacturer's instructions. Expression levels were normalized to U6 RNA.

DNA methylation assay. Genomic DNA was extracted with a QIAamp DNA Mini Kit (Qiagen Hilden, Germany) and bisulfite conversion was carried out with an Epitect Bisulfite Kit (Qiagen). DNA methylation levels were analyzed by pyrosequencing using PyroMark Q24 (Qiagen) in accordance with the manufacturer's instructions. The sequences of the primers used are shown in Table S1. As controls for human methylated and unmethylated DNAs, EpiTect methylated and unmethylated control DNAs were purchased from Qiagen. DNA extracted from normal mouse liver tissue was treated with Sss I methyl-

ase (in vitro methylated DNA: IVD), which was used as a control for mouse methylated DNA.

Luciferase promoter assay. A miR-122 promoter assay was carried out using a Dual Luciferase Reporter Assay System (Promega Madison, WI, USA). Fragments of the human miR-122 promoter with or without the DR-1 and DR-2 elements were inserted between SacI and HindIII sites within pGL4.10 (Promega). Plasmids (475 ng) with or without Sss I CpG methylase (New England Biolabs, Ipswich, MA, USA) treatment were cotransfected with a Renilla luciferase expression vector (pRL-CMV, 25 ng) into HepG2 cells using Lipofectamine 3000 (Life Technologies). Forty-eight hours after transfection, luciferase activities were measured.

Statistics. Data were analyzed using the SPSS statistical software package version 21.0. Differences at $P < 0.05$ were considered significant. All data are represented as average + SD.

Results

Clinicopathological findings in NASH-HCC model mice. To investigate the molecular mechanism underlying hepatocarcinogenesis from NASH, we used the STAM mouse, which is a simple model system using C57BL/6J mice for inducing NASH–HCC in a diabetic background through a combination of chemical and dietary interventions.[14,15] Figure 1(a) shows age-dependent changes in body and liver weight in STAM and control mice. Control mice showed age-dependent body weight gain, whereas STAM mice showed no body weight gain. The average body weight of control mice was significantly higher than that of STAM mice ($P < 0.01$). In contrast, the average liver weight in STAM mice was significantly higher than that in control mice ($P < 0.05$). STAM mice at the age of 18 weeks, which developed HCC, showed especially prominent hepatomegaly. Serum AST and ALT levels were markedly increased in STAM mice at the age of 18 weeks (Fig. 1b), suggesting that hepatocytes had been severely damaged by the development of HCC. The average levels of serum total cholesterol and triglyceride in STAM mice were significantly higher than those in control mice (Fig. 1b; $P < 0.001$ and $P < 0.05$, respectively). Hematoxylin–eosin, Azan, and Sirius red staining showed fatty liver with moderate inflammatory infiltrates including neutrophils, lymphocytes, and monocytes, and ballooning degeneration of hepatocytes at the age of 8 weeks (Fig. 2a). Azan and Sirius red staining indicated liver fibrosis at the age of 12 weeks (Fig. 2a). At the age of 18 weeks, the liver of NASH–HCC model mice macroscopically showed a granular surface and tumor protrusion (Fig. 2b). We confirmed that these tumors were pathologically compatible with HCC (Fig. 2c).

***MicroRNA-122* is downregulated in HCC derived from NASH model mice.** To determine aberrantly expressed miRNAs in HCC derived from NASH, we carried out microarray analyses using HCCs and non-tumor liver tissues in STAM mice. As shown in Figure 3(a), the results of microarray analysis indicated that some miRNAs including miR-31, miR-122, and miR-203 were downregulated in HCCs relative to non-tumor liver tissues. Among these miRNAs, we focused on miR-122, because recent studies have reported that miR-122 is the liver-specific miRNA that modulates HCV replication and is downregulated in HCCs with modulation of its target gene, cyclin G1.[18–20]

To confirm the microarray data, we carried out a TaqMan quantitative RT-PCR analysis of miR-122 expression in the liver tissues of STAM mice at the ages of 6, 8, and 12 weeks, as well as HCCs and non-tumor LC tissues at the age of
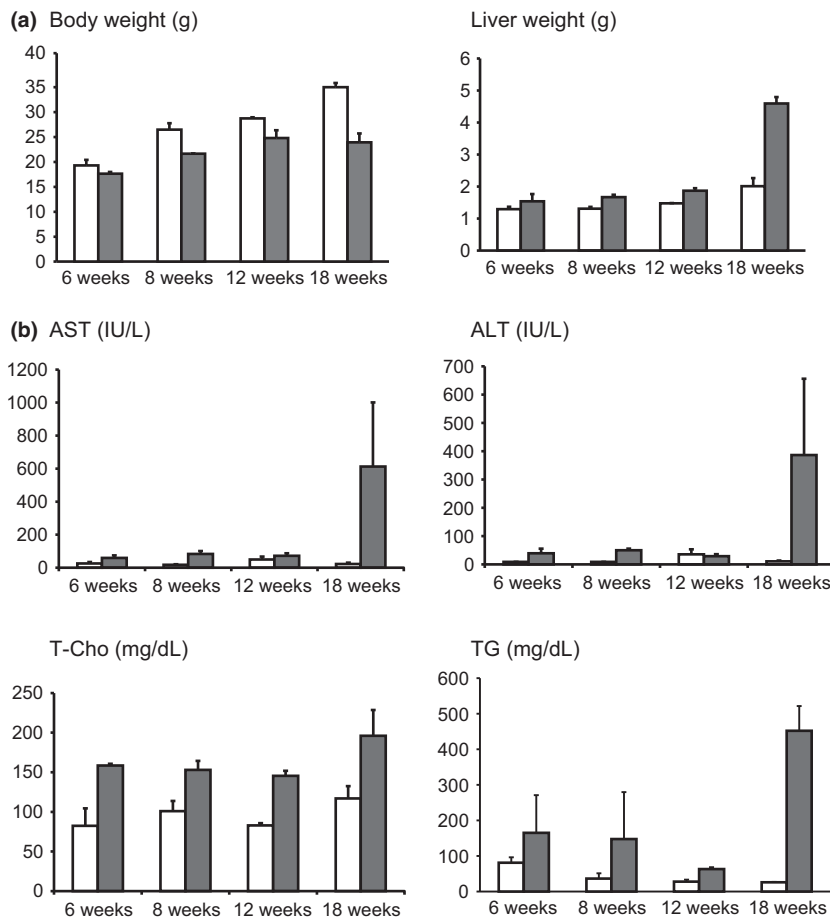
Fig. 1. Body and liver weight and biochemical examination of STAM mice. (a) Body and liver weight of control and STAM mice at the ages of 6, 8, 12, and 18 weeks. Blank and filled bars represent the average +SD of control and STAM mice, respectively. (b) Biochemical examination of serum AST, ALT, total cholesterol (T-Cho), and triglyceride (TG) in STAM mice at the ages of 6, 8, 12, and 18 weeks. Blank and filled bars represent the average ±SD for control and STAM mice, respectively.

18 weeks (Fig. 3b). There was no significant difference in *miR-122* expression among normal liver tissues of control mice and fatty liver (6 weeks), NASH (8 weeks), and LC (12 weeks) tissues in STAM mice. In contrast, *miR-122* expression in non-tumor LC at the age of 18 weeks was significantly lower than that in LC at the age of 12 weeks in STAM mice. *MicroRNA-122* expression was further decreased in HCCs relative to non-tumor LC tissues at the age of 18 weeks in STAM mice ($P < 0.05$, Fig. 3b). This result was consistent with the microarray data.

Expression levels of *miR-122* in clinical samples of HCC tissue. We examined levels of *miR-122* expression in 42 clinical samples of HCC. Specimens of HCC tissue and the surrounding non-tumor liver tissues were obtained from materials surgically resected from 42 HCC patients (HCV-positive, 22; HBV-positive, 6; non-B/non-C, 14). Histological diagnosis of NASH in the liver of HCC patients is difficult, because it is considered that liver steatosis is decreased after progression to LC and HCC. In addition, HCC patients usually require food restriction before surgery, which may reduce their liver steatosis. A previous report has graded macrovesicular steatosis from 0 to 3 based on the percentage of hepatocytes showing steatosis (0, none; 1, <33%; 2, 33–66%; 3, >66%).[17] We divided the non-B/non-C group into two according to the grade of macrovesicular steatosis in the non-tumor liver tissues. We considered grades 1–3 to be steatosis(+) ($n = 9$) and grade 0 to be steatosis(−) ($n = 5$). Figure 4(a) shows the histological appearance of non-tumor liver tissue showing steatosis in non-B/non-C patients. The liver steatosis in this case was consid-

ered to be grade 3 (macrovesicular steatosis >66%), and portal chronic inflammation and pericellular fibrosis were confirmed.

As shown in Figure 4(b), the average levels of *miR-122* expression were lower in HCC tissues than in non-tumor liver tissues in patients with HBV and HCV infection, and in non-B/non-C patients without liver steatosis. In particular, the average level of *miR-122* expression in HCCs was significantly reduced relative to the non-tumor liver tissues in HCV-positive patients ($P < 0.05$). On the other hand, *miR-122* expression in non-tumor liver tissues with steatosis in non-B/non-C patients was significantly reduced in comparison to that without steatosis ($P < 0.05$). Thus, *miR-122* expression is reduced in liver showing macrovesicular steatosis and HCCs, consistent with the findings in NASH model mice. These results suggest that *miR-122* is downregulated at the early stage during hepatocarcinogenesis from NASH.

DNA methylation status of the *miR-122* promoter region in liver cancer cell lines and HCC tissues. To reveal the molecular mechanism underlying regulation of *miR-122*, we analyzed the DNA methylation status of the *miR-122* promoter region, which contains a TATA-box, a CCAAT-box, and DR-1 and DR-2 elements[21] (Fig. 5a). We carried out the promoter assay using fragments of the human *miR-122* promoter with or without the DR-1 and DR-2 elements (Fig. 5b). Plasmids with or without Sss I CpG methylase treatment were used to cotransfect HepG2 cells with the *Renilla* luciferase expression vector. Forty-eight hours after transfection, luciferase activities were measured. The relative luciferase activity of the construct containing the DR-1 and DR-2 elements was significantly higher
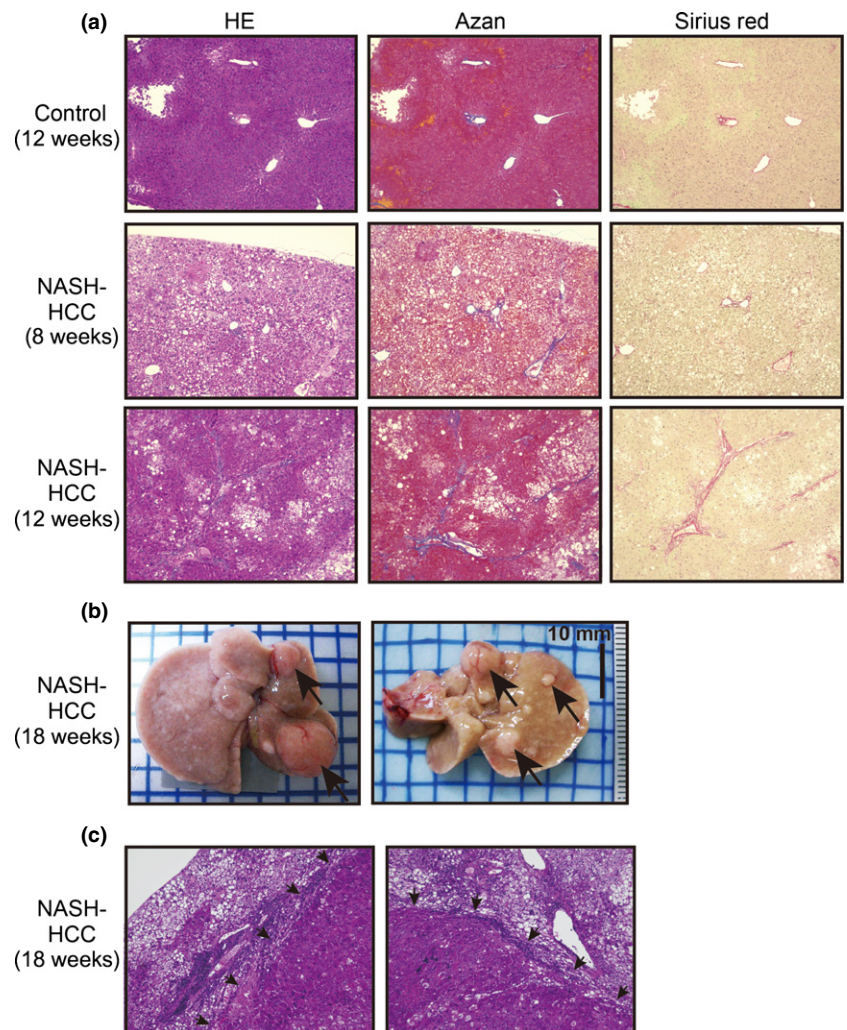
Fig. 2. Histopathological images of the liver of STAM mice. (a) Histopathological images in the liver of control (12 weeks) and STAM mice (8 and 12 weeks). Hematoxylin–eosin (HE), Azan, and Sirius red staining showed fatty liver with moderate inflammatory infiltrate include neutrophils, lymphocytes, and monocytes, and ballooning degeneration of hepatocytes in STAM mice at the age of 8 weeks. Azan and Sirius red staining showed liver fibrosis in STAM mice at the age of 12 weeks. (b) Macroscopic appearance of the liver in STAM mice at the age of 18 weeks. The liver of STAM mice showed a granular surface and tumor protrusion. (c) HE staining of the liver in STAM mice at the age of 18 weeks. Tumors are pathologically compatible with hepatocellular carcinoma (HCC) (arrows). NASH, non-alcoholic steatohepatitis.
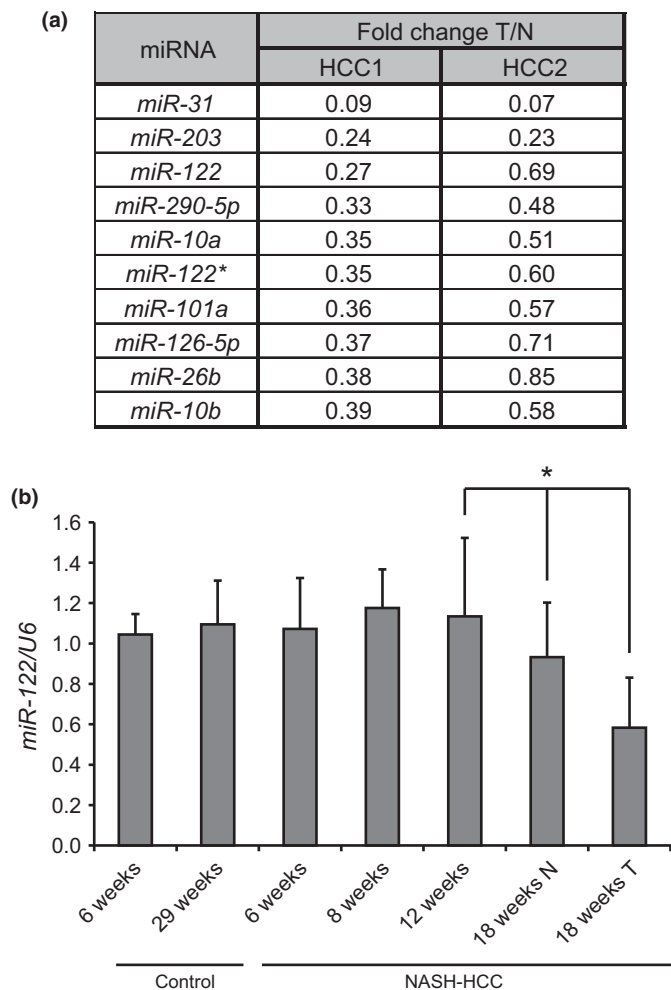
than that of the construct lacking these elements (*$P < 0.01$, Fig. 5b). After treatment with CpG methylase, the relative luciferase activities were significantly decreased in the constructs both with and without the DR-1 and DR-2 elements (**$P < 0.005$, Fig. 5b). These results indicate that the DR-1 and DR-2 elements in the *miR-122* promoter are essential for regulation of *miR-122* expression and that DNA methylation around the DR-1 and DR-2 elements suppress *miR-122* expression.

We analyzed the DNA methylation status of human HCC samples by bisulfite pyrosequencing. For this, we designed three sets of primers (P1, P2, and P3) to determine DNA methylation status at the CpG sites, indicated by asterisks in Figure 5(a). As shown in Figure 6(a), the levels of DNA methylation in the P1 and P2 regions were very high in both HepG2 and HuH7 cells, and were decreased to ~70% after treatment with 5-Aza-CdR. The P3 region was not methylated in HuH7 cells, whereas it was highly methylated in HepG2 cells, and was decreased to ~60% after 5-Aza-CdR treatment. The expression level of *miR-122* was much higher in HuH7 cells than in HepG2 cells (Fig. 6b). The expression of *miR-122* was significantly increased after 5-Aza-CdR treatment in HepG2 cells, whereas there was no significant difference after 5-Aza-CdR treatment in HuH7 cells (Fig. 6b). These findings indicate that DNA methylation of the P3 region is critical for regulation of *miR-122* expression.

We next examined DNA methylation levels in samples of human HCC with different types of etiology, as shown in Figure 6(c). DNA methylation levels in samples of human HCC tissue were lower (~30%) than those in non-tumor liver tissues in all regions of the *miR-122* promoter. In particular, the average levels of DNA methylation in the *miR-122* promoter region were significantly reduced in HCC tissues relative to non-tumor liver tissues in non-B/non-C patients without liver steatosis and in HCV-positive patients (Fig. 6c). We also examined levels of DNA methylation in the *miR-122* promoter region in non-tumor LC tissues and HCCs of STAM mice, as well as normal liver tissues obtained from C57BL/6J mice. As shown in Figure 6(d), there was no significant difference in the level of DNA methylation between non-tumor LC and HCC. These findings suggest that silencing of *miR-122* expression during hepatocarcinogenesis is not mediated by DNA hypermethylation in the promoter region.
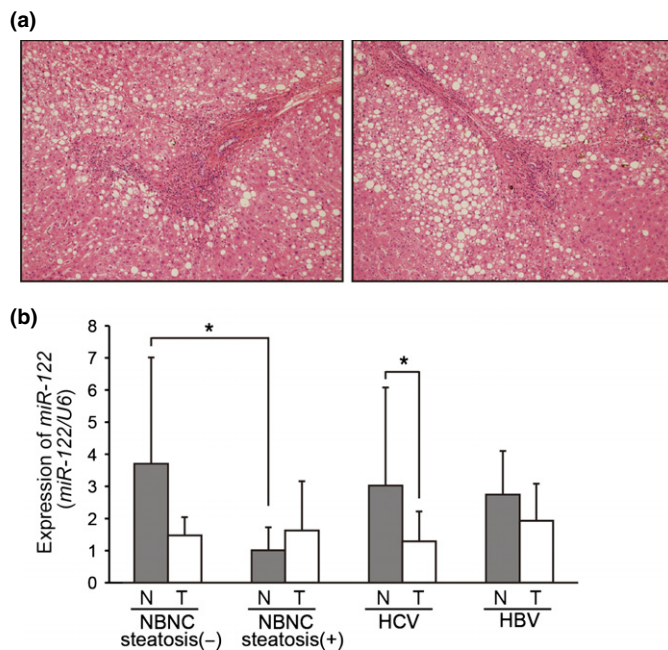
Discussion

MicroRNA-122 is the most abundant miRNA in the liver and is implicated in several important aspects of liver pathogenesis, including HCV replication, lipid metabolism, and development of HCC. *MicroRNA-122* is known to bind to the 5′-UTR of the HCV genome and promotes HCV replication. The inhibitor

(a)

miRNA	Fold change T/N	
	HCC1	HCC2
miR-31	0.09	0.07
miR-203	0.24	0.23
miR-122	0.27	0.69
miR-290-5p	0.33	0.48
miR-10a	0.35	0.51
*miR-122**	0.35	0.60
miR-101a	0.36	0.57
miR-126-5p	0.37	0.71
miR-26b	0.38	0.85
miR-10b	0.39	0.58

(b)

(a)

(b)

Fig. 4. Levels of *microRNA-122* (*miR-122*) expression in clinical samples obtained from hepatocellular carcinoma (HCC) patients. (a) Histopathological images (HE staining, ×100) of non-tumor liver tissue from a hepatitis B virus-negative/hepatitis C virus-negative (NBNC) HCC patient, showing steatosis. This case was considered to be grade 3 (macrovesicular steatosis >66%), with chronic portal inflammation and pericellular fibrosis. (b) The average levels of *miR-122* expression in HCC tissues (T, clear bars) and non-tumor liver tissues (N, filled bars). Tissue specimens of HCC and the surrounding non-tumor liver were obtained from patients with NBNC HCC with or without liver steatosis, as well as patients with hepatitis C virus-positive and hepatitis B virus-positive HCC. *miR-122* expression is normalized with U6. *$P < 0.05$.

Fig. 3. Expression profiles of microRNAs (miRNAs) in the liver of STAM mice. (a) Microarray analyses of miRNA expression profile in hepatocellular carcinoma (HCC) tissues (T) compared with non-tumor liver tissues (N) in two STAM mice at the age of 18 weeks (HCC1 and HCC2). (b) *MicroRNA-122* (*miR-122*) expression in the liver of control (6 and 29 weeks) and STAM mice (6, 8, 12, and 18 weeks). *miR-122* expression normalized with U6 is represented as average +SD. Downregulation of *miR-122* in the liver of STAM mice from the age of 12–18 weeks for non-tumor (N) and HCC (T) was significant (*$P < 0.05$).

of *miR-122* decreases HCV RNA levels in patients with chronic HCV genotype 1 infection.[22] Downregulation of *miR-122* expression has been reported in patients with HCC.[19,20] Hsu *et al.*[23] have shown that deletion of *miR-122* results in hepatosteatosis, hepatitis, and the development of HCCs.

Our present results indicated that there was no change in *miR-122* expression during progression from normal liver to NALFD (6 weeks), NASH (8 weeks), and LC (12 weeks) in STAM mice. However, *miR-122* expression in non-tumor LC at the age of 18 weeks was significantly lower than that in LC at the age of 12 weeks in STAM mice. Expression of *miR-122* was further decreased in HCCs relative to non-tumor LC tissues at the age of 18 weeks in STAM mice. These results strongly suggested that suppression of *miR-122* is critical for the initiation and development of NASH-derived HCC. We also confirmed *miR-122* expression in clinical samples obtained from patients with HCC. Expression of *miR-122* was

reduced in liver showing macrovesicular steatosis and HCC, consistent with the findings in the NASH model mice. These results suggest that silencing of *miR-122* is an early event during hepatocarcinogenesis from NASH.

Recent studies have shown that peroxisome proliferator activated receptor-gamma (PPAR-γ) is associated with the DR-1 and DR-2 consensus sites in the *miR-122* promoter, and that epigenetic alterations in the promoter region play important roles in the regulation of *miR-122* expression.[24,25] In general, DNA hypermethylation at the CpG island promoter leads to silencing of tumor suppressor genes. The *miR-122* promoter region is CpG-poor, but the results of our promoter assay indicated that DNA methylation around the DR-1 and DR-2 elements suppressed *miR-122* expression. Unexpectedly, our analyses revealed that DNA methylation levels in human HCC tissue samples were lower (~30%) than in non-tumor liver tissues in all regions of the *miR-122* promoter, although *miR-122* expression was downregulated. We also examined the DNA methylation status of the *miR-122* promoter region in HCCs and non-tumor LC tissues in STAM mice. The levels of *miR-122* methylation in HCCs and non-tumor LC tissues in STAM mice were around 30%, and there was no significant difference between them. These findings suggest that silencing of *miR-122* during hepatocarcinogenesis is not mediated by DNA hypermethylation in the promoter region. Further studies are necessary to identify the factors that inhibit *miR-122* expression during hepatocarcinogenesis from NASH.

(a)

```
-496 GAATGCATGGTTAACTACGTCAGAAATGACCAGTTCAAGAGGAGAATGAGATTGGCTTCCAAATGTTGGTCAAGAG
        P1 *                                                          P2 *
-420 CTCTACGTAGCATGAGCCAAGGATCTATTGAACTTAGTAGGCTCCTGTGACCGGTGACTCTTCTGTCTCTAGAAATC
                                                          P3 *              DR-1
-343 TGGGGAGGTGACCAGGTCATACATGGCAGTCTTCCCGTGAGGAACGTTAAACTGGTTGGAAGTTGGGGTTCTGAG
        DR-2
-268 GGGAAGATGTATTCACTAGGTGACCTGTCTTCTCTGCCTCGGTGGCCTCCATGGCTGCCTGCTGGCCGCACACCC
-193 CCACTCAGCAGAGGAATGGACTTTCCAATCTTGCTGAGTGTGTTTGACCAAAGGTGGTGCTGACTTAGTGGCCTAA
                              CCAAT-box                                        DR-1
-117 GGTCGTGCCCTCCCTCCCCCACTGAATCGATAAATAATGCGACTTATCAGAAAGAGAAAGAATTGTTTACTTTTAAA
        ↳TSS
-40  CCCTGGATCCCATAAAGGGAGAGGGGAGAGGCCTAAAGCCACAGAAGCTGT
              TATA-box
```

(b)

Fig. 5. Promoter assay of *microRNA-122* (*miR-122*) expression. (a) The promoter region of *miR-122*, which contains a TATA-box, a CCAAT-box, and DR-1 and DR-2 elements. DNA methylation status was determined by bisulfite pyrosequencing at the CpG sites indicated by asterisks. Arrow indicates the transcription start site (TSS), as described previously.[21] (b) Promoter assay of *miR-122* expression using a Dual Luciferase Reporter Assay System. Fragments of the human *miR-122* promoter with or without the DR-1 and DR-2 elements were inserted between the *Sac*I and *Hind*III sites within pGL4.10. Plasmids with or without Sss I CpG methylase treatment were cotransfected with *Renilla* luciferase expression vector into HepG2 cells. Forty-eight hours after transfection, luciferase activities were measured. *$P < 0.01$; **$P < 0.005$.
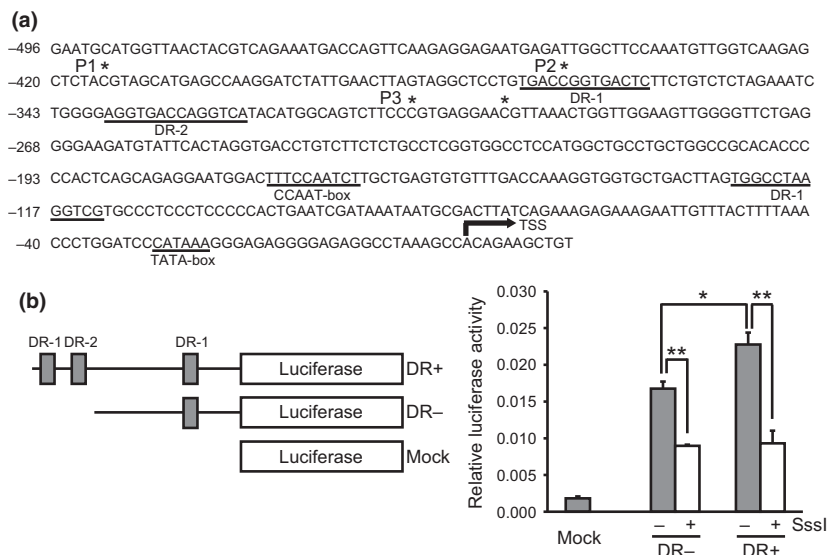
Fig. 6. DNA methylation status of the promoter region of *microRNA-122* (*miR-122*) in liver cancer cell lines and hepatocellular carcinoma (HCC) tissues. (a) DNA methylation levels of the *miR-122* promoter region in HepG2 and HuH7 cells treated with 1 or 3 μM 5-aza-2′-deoxycytidine (5AZA). Methylated (MC) and unmethylated (UC) control DNAs were used as controls. (b) Average levels of *miR-122* expression in HepG2 and HuH7 cells treated with 5AZA. *miR-122* expression is normalized with U6. *$P < 0.05$. (c) Levels of DNA methylation in the *miR-122* promoter region in HCC tissues (T, white columns) and non-tumor liver tissues (N, filled columns). Tissue specimens of HCC and the surrounding non-tumor liver were obtained from patients with hepatitis B virus-negative/hepatitis C virus-negative (NBNC) HCC with or without liver steatosis, as well as from patients with hepatitis C virus-positive and hepatitis B virus-positive HCC. Methylated (MC) and unmethylated (UC) control DNAs were used as controls. *$P < 0.005$. (d) Levels of DNA methylation in the *miR-122* promoter region in non-tumor liver tissues (NT) and HCCs of STAM mice. Normal liver tissues obtained from C57BL/6J mice were used as a control (Cont). DNA from normal mouse liver treated with Sss I methylase (*in vitro* methylated DNA [IVD]) was used as a control for methylated DNA.
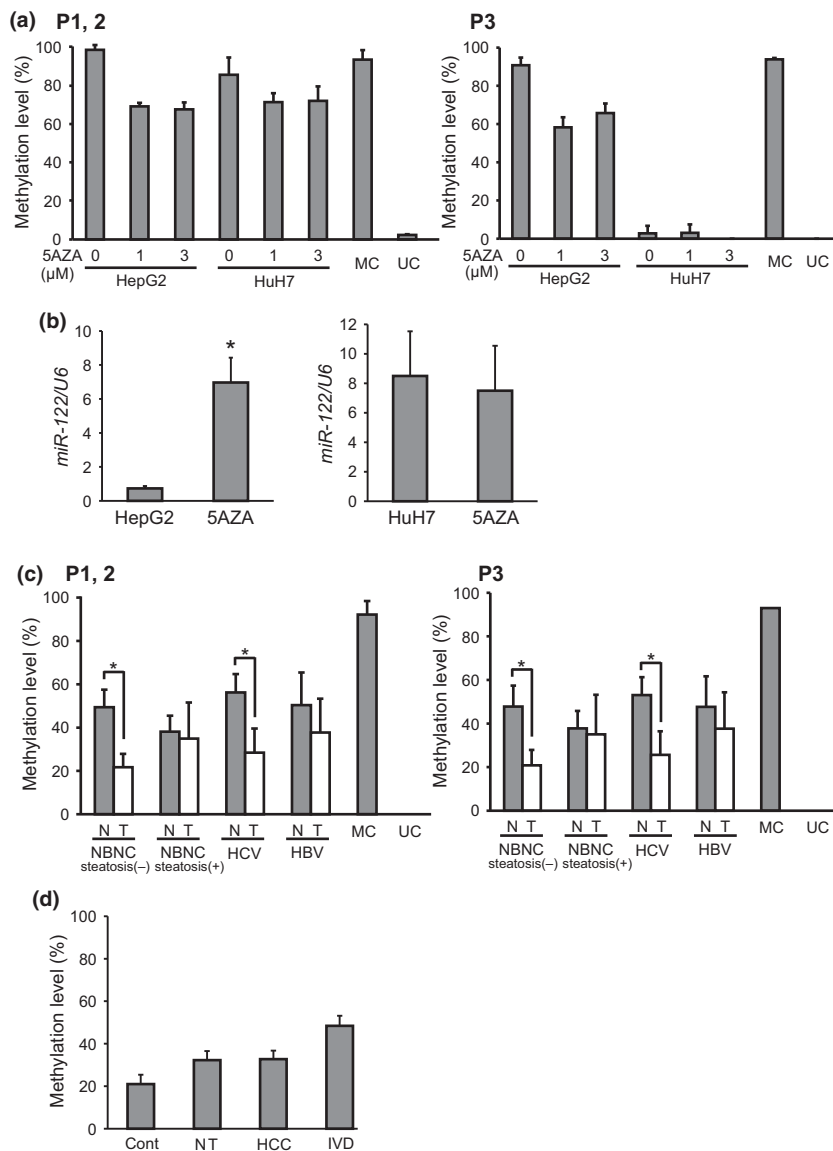
In summary, our present results indicate that the tumor suppressor *miR-122* is downregulated at an early stage of hepatocarcinogenesis from NASH in both an animal model and samples of human tissue. Silencing of *miR-122* in the steatotic liver may play an important role in the initiation of HCC through modulation of its target genes. These novel findings suggest that *miR-122* could be used as a molecular marker for evaluating the risk of HCC, and as a therapeutic target for HCC, in patients with NASH.

Disclosure Statement

The authors have no conflict of interest.

Abbreviations

5-Aza-CdR	5-aza-2′-deoxycytidine
HBV	hepatitis B virus
HCC	hepatocellular carcinoma
HCV	hepatitis C virus
LC	liver cirrhosis
miRNA	microRNA
NASH	non-alcoholic steatohepatitis
NAFLD	non-alcoholic fatty liver disease
NBNC	hepatitis B virus-negative/hepatitis C virus-negative

References

1 Farazi PA, DePinho RA. Hepatocellular carcinoma pathogenesis: from genes to environment. *Nat Rev Cancer* 2006; **6**: 674–87.
2 El-Serag HB. Hepatocellular carcinoma. *N Engl J Med* 2011; **365**: 1118–27.
3 Ascha MS, Hanouneh IA, Lopez R, Tamimi TA, Feldstein AF, Zein NN. The incidence and risk factors of hepatocellular carcinoma in patients with nonalcoholic steatohepatitis. *Hepatology* 2010; **51**: 1972–8.
4 Michelotti GA, Machado MV, Diehl AM. NAFLD, NASH and liver cancer. *Nat Rev Gastroenterol Hepatol* 2013; **10**: 656–65.
5 Starley BQ, Calcagno CJ, Harrison SA. Nonalcoholic fatty liver disease and hepatocellular carcinoma: a weighty connection. *Hepatology* 2010; **51**: 1820–32.
6 He L, Hannon GJ. MicroRNAs: small RNAs with a big role in gene regulation. *Nat Rev Genet* 2004; **5**: 522–31.
7 Rottiers V, Naar AM. MicroRNAs in metabolism and metabolic disorders. *Nat Rev Mol Cell Biol* 2012; **13**: 239–50.
8 Calin GA, Croce CM. MicroRNA signatures in human cancers. *Nat Rev Cancer* 2006; **6**: 857–66.
9 Croce CM. Causes and consequences of microRNA dysregulation in cancer. *Nat Rev Genet* 2009; **10**: 704–14.
10 Saito Y, Liang G, Egger G et al. Specific activation of microRNA-127 with downregulation of the proto-oncogene BCL6 by chromatin-modifying drugs in human cancer cells. *Cancer Cell* 2006; **9**: 435–43.
11 Saito Y, Friedman JM, Chihara Y, Egger G, Chuang JC, Liang G. Epigenetic therapy upregulates the tumor suppressor microRNA-126 and its host gene EGFL7 in human cancer cells. *Biochem Biophys Res Commun* 2009; **379**: 726–31.
12 Saito Y, Suzuki H, Tsugawa H et al. Chromatin remodeling at Alu repeats by epigenetic treatment activates silenced microRNA-512-5p with downregulation of Mcl-1 in human gastric cancer cells. *Oncogene* 2009; **28**: 2738–44.
13 Saito Y, Suzuki H, Taya T et al. Development of a novel microRNA promoter microarray for ChIP-on-chip assay to identify epigenetically regulated microRNAs. *Biochem Biophys Res Commun* 2012; **426**: 33–7.
14 Kawai D, Takaki A, Nakatsuka A et al. Hydrogen-rich water prevents progression of nonalcoholic steatohepatitis and accompanying hepatocarcinogenesis in mice. *Hepatology* 2012; **56**: 912–21.
15 Fujii M, Shibazaki Y, Wakamatsu K et al. A murine model for non-alcoholic steatohepatitis showing evidence of association between diabetes and hepatocellular carcinoma. *Med Mol Morphol* 2013; **46**: 141–52.
16 Sugiishi A, Kimura M, Kamiya R et al. Derangement of ghrelin secretion after long-term high-fat diet feeding in rats. *Hepatol Res* 2013; **43**: 1105–14.
17 Brunt EM, Janney CG, Di Bisceglie AM, Neuschwander-Tetri BA, Bacon BR. Nonalcoholic steatohepatitis: a proposal for grading and staging the histological lesions. *Am J Gastroenterol* 1999; **94**: 2467–74.
18 Jopling CL, Yi M, Lancaster AM, Lemon SM, Sarnow P. Modulation of hepatitis C virus RNA abundance by a liver-specific MicroRNA. *Science* 2005; **309**: 1577–81.
19 Gramantieri L, Ferracin M, Fornari F et al. Cyclin G1 is a target of miR-122a, a microRNA frequently down-regulated in human hepatocellular carcinoma. *Cancer Res* 2007; **67**: 6092–9.
20 Fornari F, Gramantieri L, Giovannini C et al. MiR-122/cyclin G1 interaction modulates p53 activity and affects doxorubicin sensitivity of human hepatocarcinoma cells. *Cancer Res* 2009; **69**: 5761–7.
21 Li ZY, Xi Y, Zhu WN et al. Positive regulation of hepatic miR-122 expression by HNF4alpha. *J Hepatol* 2011; **55**: 602–11.
22 Janssen HL, Reesink HW, Lawitz EJ et al. Treatment of HCV infection by targeting microRNA. *N Engl J Med* 2013; **368**: 1685–94.
23 Hsu SH, Wang B, Kota J et al. Essential metabolic, anti-inflammatory, and anti-tumorigenic functions of miR-122 in liver. *J Clin Invest* 2012; **122**: 2871–83.
24 Jung CJ, Iyengar S, Blahnik KR et al. Epigenetic modulation of miR-122 facilitates human embryonic stem cell self-renewal and hepatocellular carcinoma proliferation. *PLoS ONE* 2011; **6**: e27740.
25 Song K, Han C, Zhang J et al. Epigenetic regulation of MicroRNA-122 by peroxisome proliferator activated receptor-gamma and hepatitis b virus X protein in hepatocellular carcinoma cells. *Hepatology* 2013; **58**: 1681–92.

Supporting Information

Additional supporting information may be found in the online version of this article:

Table S1. Sequences of primers used for pyrosequence of the *miR-122* promoter region.